Experimental Comparison of Observer-Based Friction Compensation Schemes for an Electromechanical Positioning System

H.Henrichfreise and C. Witte
Cologne Laboratory of Mechatronics
Polytechnic Cologne
henrichfreise@kt.fh-koeln.de

Introduction

In high precision positioning applications, tracking accuracy requirements render friction compensation indispensable. Many methods have been developed to compensate friction torques and forces acting at positioning devices. The issue of this paper is the comparison of different compensation schemes based on LQG control.

While section 1 introduces the position control system, section 2 presents the different friction compensation schemes. Emphasis is laid on their practical use by showing experimental results of the tracking behaviour with typical reference profiles. Section 2 also addresses robustness against noise and modelling errors, undesired phenomena from nonlinear plant characteristics, and external disturbances. On this basis a concluding assessment is given in section 3.

1. Electromechanical positioning system and control

Figure 1 shows the setup of the electromechanical positioning system (EMPS) which is the plant in this context. A flexible coupling between the drive and load side with only approximately known stiffness and damping produces a mechanical resonance at a frequency of about 100 Hz. A backlash-free ball screw unit which produces a relatively high friction torque serves as a gear from screw revolution to carriage displacement. Additional friction has been introduced by a friction wheel to improve the clearness of the experimental results. If not appropriately compensated for, the resulting friction torque will cause considerable positioning errors.
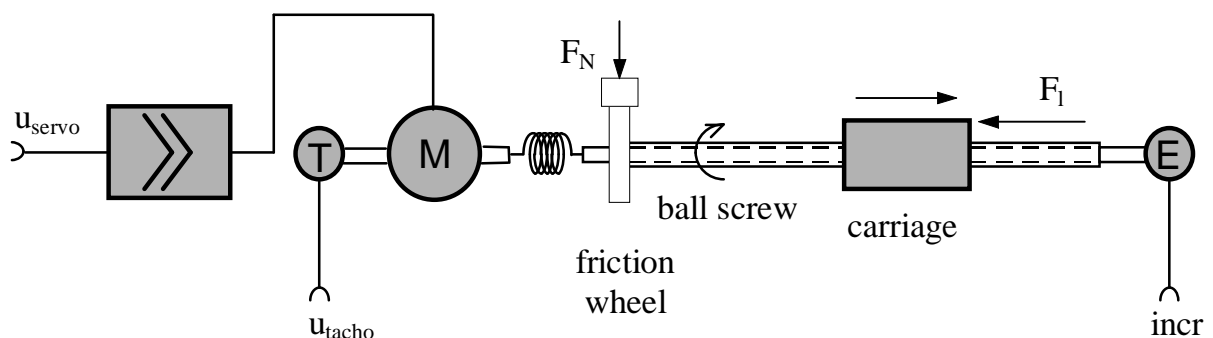

Fig. 1 *Electromechanical positioning system (EMPS)*

Figure 2 presents a measurement of the friction torque (load-side plus drive-side) over carriage velocity, with dominant kinetic (Coulombic) and viscous friction at high velocities, and a hint of boundary friction at low velocities and hysteresis from frictional memory [4]. The maximum friction torque is about 20% of the maximum motor torque of 0.1575 Nm.
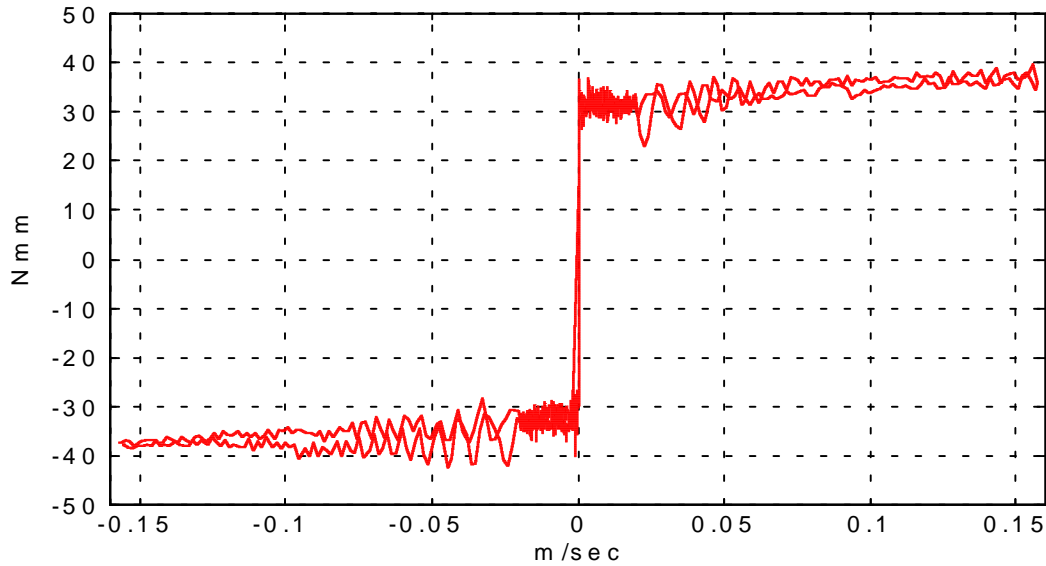
Fig. 2 *Friction torque in the EMPS*

Another source of position errors is the load force F_l acting at the carriage, which is contained in the disturbance input vector $\underline{u}_{pd}$ to the plant subsystem from figure 3.

LQG control was selected for high bandwidth position control. It contains a linear quadratic regulator (LQR) for feedback of the EMPS states, the drive-side and load-side angular displacements and velocities, and the torque generated by the DC motor. These states are reconstructed by a linear observer designed as a linear quadratic estimator (LQE). Its inputs from the plant measurement vector $\underline{y}_{pm}$ are the output voltage u_{tacho} of a DC tachometer attached to the motor shaft and the load-side angular displacement supplied by the counter value incr of an incremental encoder. The resolution of the digital position measurement equals a carriage displacement of 1.25 μm. The control signal is the input voltage u_{servo} to the current-controlled servo amplifier.

A coarse structure of the control loop with EMPS, LQG compensator and reference profile generator is given in figure 3.
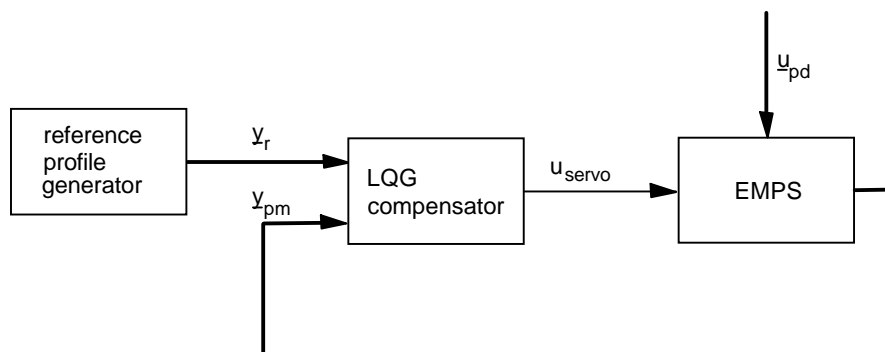

Fig. 3 *Control structure for the EMPS*

The internal structure of the compensator subsystem depends on the scheme used for friction compensation from section 2. Common to all structures is the usage of reference signals, the plant state feedback, and the design procedure.

The output $\underline{y}_r$ of the reference profile generator provides the reference time histories for the load-side angular position, velocity, and acceleration. They are fed forward to the control signal to achieve a steady-state accurate carriage position for up to parabolic position profiles. The corresponding feedforward gains were determined with the LQR design for the plant state feedback by augmenting the linear plant model with an appropriate reference model, where the position, velocity and acceleration errors of the carriage and the control signal were used as objective variables in the LQR cost function. The reciprocal values of the allowed (desired) variances of these variables served as the design parameters in the corresponding weighting matrices. Robustness against disturbances and uncertainties in the plant control input path is crucial for a successful compensator implementation. This was aspired with trying to achieve Input Loop Transfer Recovery (LTR) [1] by using suitable noise intensities as design parameters in the LQE design. For more details on the control design the reader may refer to [2].

All compensators from section 2 were designed in the continuous time domain and discretized for implementation using MATLAB and the Control System Toolbox, followed by an analysis of robustness to parameter variations, noise and implementation effects by simulation of the closed-loop system from figure 3 with discrete compensator and nonlinear plant model with SIMULINK. If it had turned out to be worth, a compensator together with the reference profile generator was digitally implemented for experimentation using the dSPACE TDE [3]. A sampling period of 300μs turned out to be sufficient to cover the fastest closed-loop system modes.

Two sets of reference time histories called track I and track II are used to investigate the performance of the different friction compensation schemes. They are shown in figures 4 and 5 scaled to the position, velocity and acceleration on the carriage side. Both tracks require a control signal close to the servo amplifier saturation bounds. While track I represents simple uni-directional motion, track II contains a motion reversal which, due to the sign change of static friction with the velocitiy crossing zero (see figure 2), is more demanding for precise position control with friction.
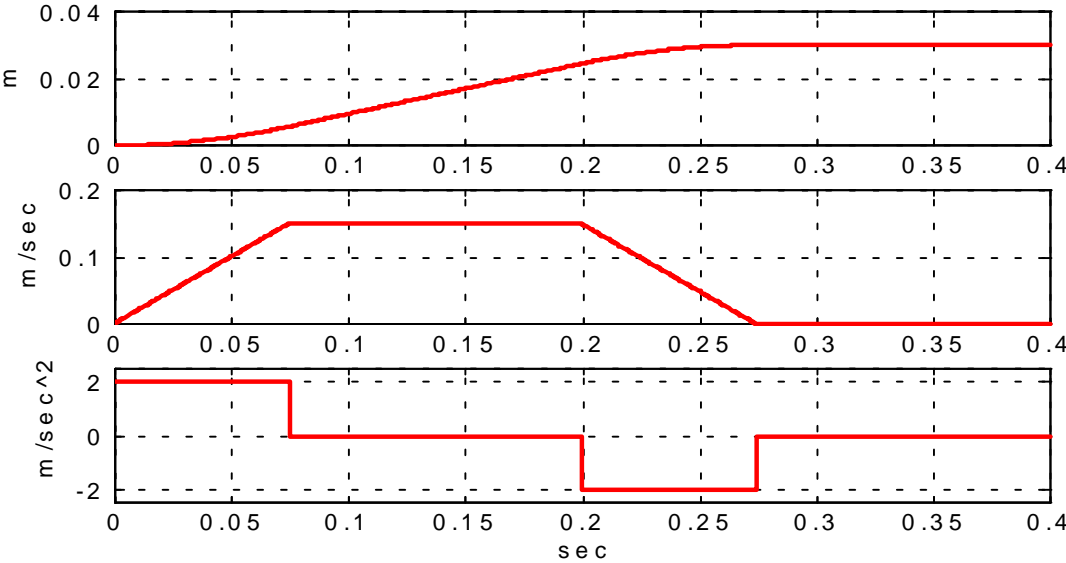

Fig. 4 *Carriage reference position, velocity, and acceleration for track I*
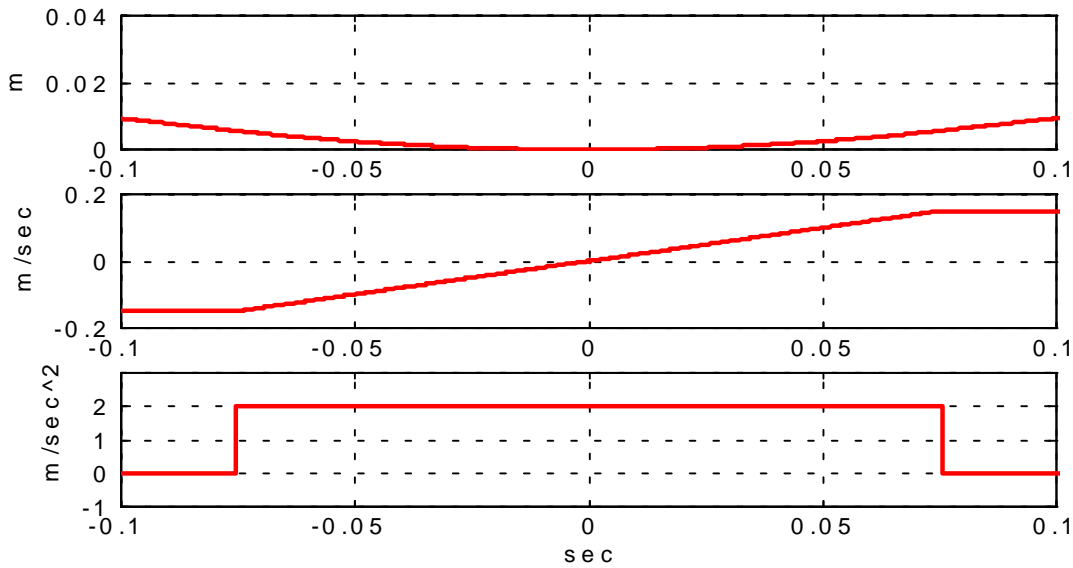
Fig. 5 *Carriage reference position, velocity, and acceleration for track II*

These tracks commanded to a LQG control with feedback of the EMPS states and feedforward of the reference signals, but without any friction compensation, resulted in the position error measurements presented in figure 6.
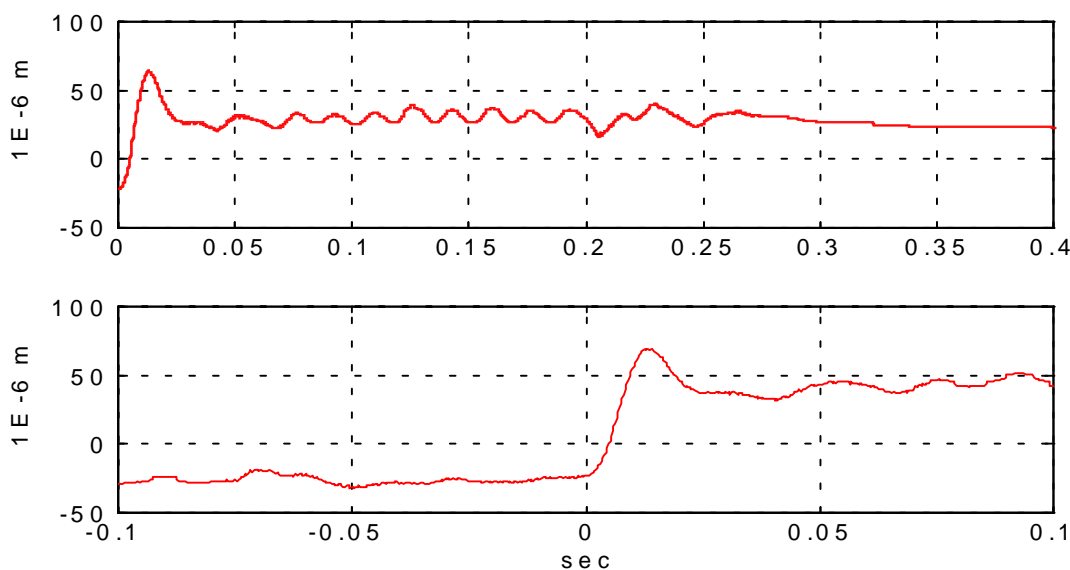

Fig. 6 *Positioning errors without disturbance compensation for track I (top) and track II (bottom)*

It was found by simulation which yielded results very close to the above measurements that friction is the only source of the significant steady-state positioning errors in all tracking phases. Thus, the compensation of friction is indispensable. The different compensation schemes added to the above LQG control will be discussed in the following section.

2. Friction compensation

Various approaches to reduce friction-dependent position errors can be found in the literature [4]. This paper concentrates on observer-based schemes on the basis of the LQG control mentioned in section 1. Its gain matrices $\underline{K}_r$ for feedforward of the reference input and $\underline{K}_p$ for the feedback of the plant state estimate $\underline{x}_{ep}$ (see figure 7) are contained in all investigated schemes. These schemes originate from the basic LQG control structure by augmentations ranging from simple integral feedback of the position error (PI state feedback) to model-based estimation and compensation. Experimental results and a discussion of robustness issues for the resulting overall compensators are given in the following subsections.

2.1 Integral feedback of the position error

Integral feedback is a simple and widespread measure to cope with steady-state errors. Its main advantage is that it counteracts against all errors which become visible in the controlled variable at the integrator input, regardless whether they are caused by external disturbance inputs, nonlinear plant behaviour, or parameter variations. Therefore integral feedback is particularly suitable if the sources of errors are not well known or are not easy to model. Figure 7 shows the compensator structure for friction compensation with integral feedback of the load-side angular position error e_φ , which is the difference of the reference angle φ_r and the load-side angular displacement φ_l of the screw. The gain K_I has been calculated during the LQR design by using an augmented plant model providing the integral of the load-side position error as an output variable. This variable had been added to the list of objective variables for design and weighted by a suitable entry to the corresponding element of the output weighting matrix [5]. While it should be as high as possible for good disturbance rejection, the value of the weighting element as design parameter is limited by an increasingly noisy control and position signal. The observer for the plant states is given with equation (C1) from the appendix and the observer gain matrix from LQE design.
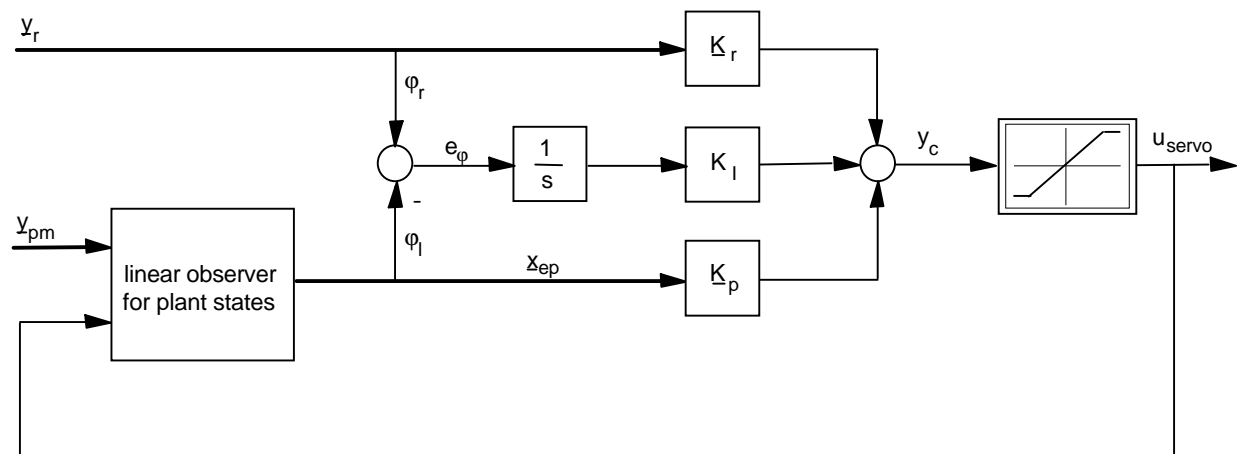

Fig. 7 *Compensator with integral feedback of position error*

Figure 8 shows the measurements of the positioning errors with the integral control. Friction compensation and steady-state accuracy is achieved for both track I and II. The error reaches its maximum after rapid changes of friction when the drive starts to move with high acelleration from standstill (track I) or changes its direction of motion (track II).
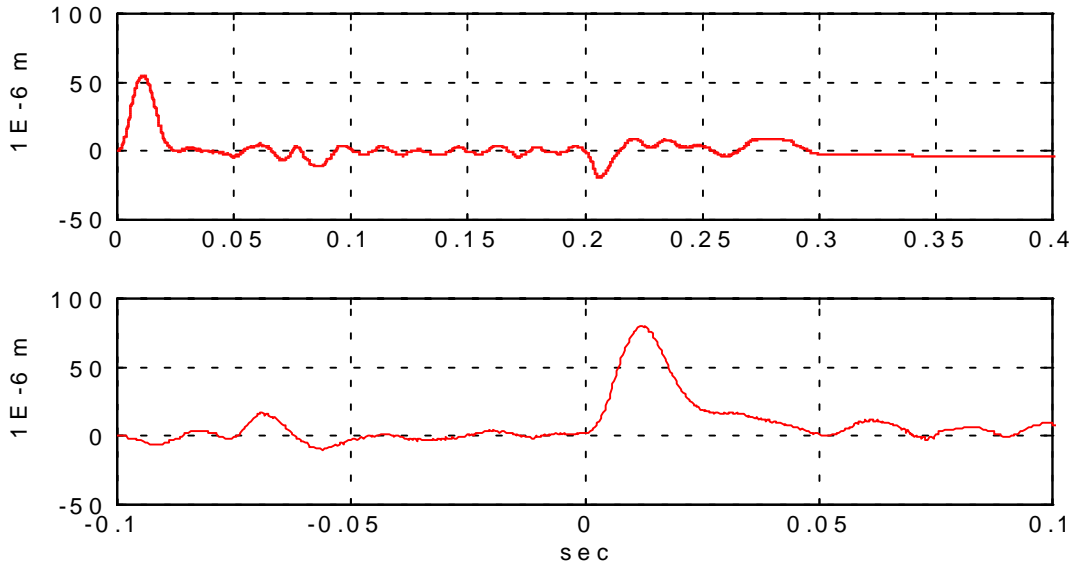
Fig. 8 *Positioning errors for track I (top) and II (bottom), compensator with integral feedback of position error*

The achieved grade of LTR of this LQG control can be checked by its open-loop bode plots. For this, the control loop from figure 3 with all linear subsystems (without saturation and friction) has to be cut directly at the plant input, leading to a wrong input (the compensator output instead of the plant control input) to the observer in figure 7. The open-loop bode plots of the transfer path from the plant control input to the compensator output of this system have to be compared to those of a system without an observer where all states are assumed to be measurable, i.e. with LQR for static state feedback only. Since LQR control is robust providing an infinite gain margin and a significant phase margin, the dynamic state feedback with LQG compensator will be robust if its loop transfer, given by the open-loop bode plots, at least around crossover is close to recover that of the LQR-controlled system.
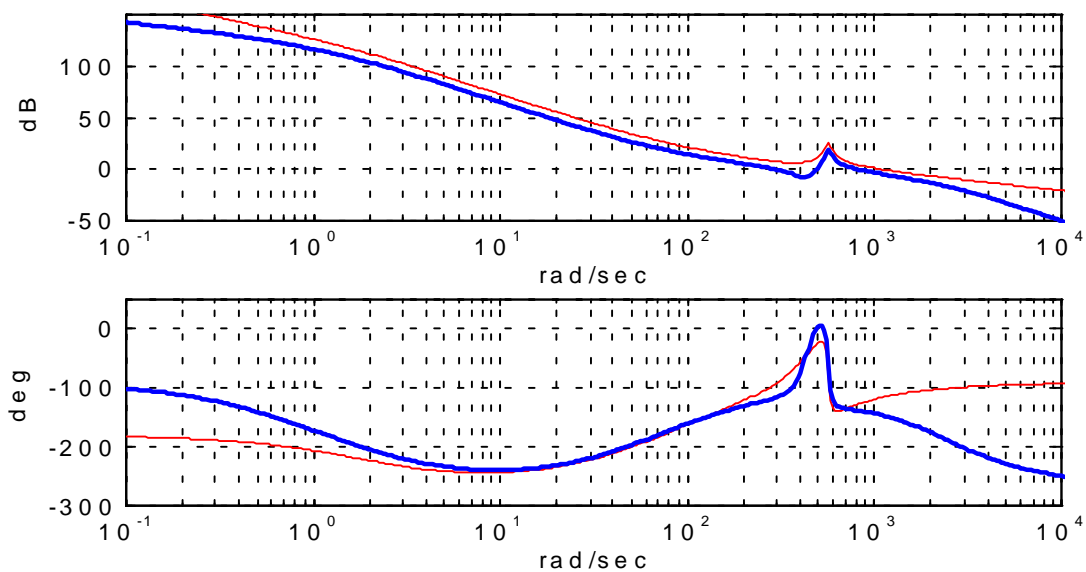

Fig. 9 *Open-loop bode plots for system with LQR (thin lines) and compensator (bold lines) with integral feedback of position error*

As it becomes clear from figure 9, the compensator from figure 7 (without saturation) provides a good LTR and robustness of the linear control system against disturbances and uncertainties in the plant control input path. Full LTR with identical bode plots can only be achieved with the observer gains tending to infinity [6] which is only of theoretical use.

As known from the literature, e.g. [7], integral control may lead to limit cycles for the nonlinear system when high static friction and a rapid transition to a lower kinetic friction are present. These conditions are not given with the friction characteristic of the EMPS from figure 2. Even with unfavourable friction parameters in simulation it was not possible to produce a limit cycle with the integral position error feedback.
More simulation of the nonlinear control system with changing load-side inertia and stiffness of the coupling between drive and load in a range of ±20 % revealed a high grade of robustness against variation of these parameters which are also uncertain in practice.

A drawback of the control with integral feedback of the position error is that it shows an undesirably weak response to disturbing forces F_l . This becomes especially clear in the experiment when the ball screw is manually twisted, but can also be recognized in simulation. Figure 10 gives a simulation result for a force step of 150 N at 0.01 sec applied to the input F_l . The weak disturbance rejection is indicated by the slow decay of the position error.
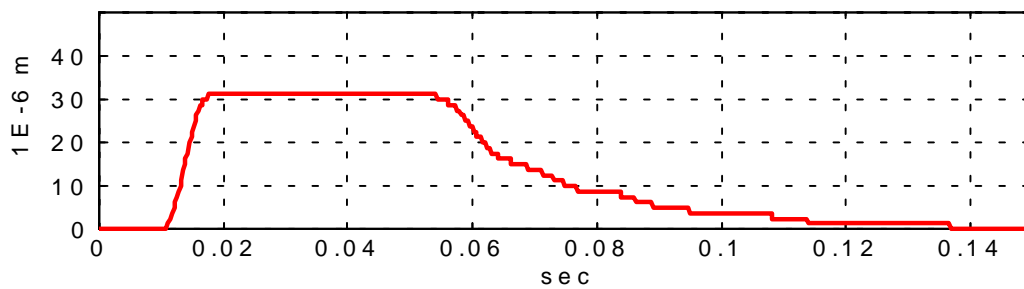

Fig. 10 *Position error for force step input, compensator with integral feedback of position error*

An attempt to improve this disturbance rejection by a stronger integral feedback with increasing the weighting of the position error integral in the LQR design resulted in a poor robustness and, finally, in an unstable control system. This came along with an increasingly noisy control and position signal in the experiment.

2.2 Linear model-based disturbance estimation and feedforward

If control errors originate from an external input signal, another method for compensation is a suitable feedforward of this input to the control signal. For linear control design with a linearized plant model, Coulombic friction can well be modelled by a constant external disturbance input to the plant. Because this input cannot be measured, an estimate is required for feedforward. This can be provided by an observer which is designed for the linear plant model augmented by a suitable dynamic model at the disturbance input (see appendix A). A good choice to model Coulombic friction as a constant external input is a simple integrator with appropriate initial condition. With this model for the dominant load-side friction torque as an element of the plant disturbance input vector $\underline{u}_{pd}$, the LQE design for the EMPS yields an augmented plant observer whose additional disturbance model state x_{ed} provides an estimate for the friction torque. The corresponding feedforward gain K_d to compensate the friction-dependent position error is computed with the LQR design for the augmented plant model.

Figure 11 illustrates the resulting compensator structure, where the observer for the plant and disturbance states is given by equations (A4a-c) in the appendix. Since this disturbance estimation does not differ friction from other disturbing torques at the load side, the scheme also compensates position errors due to the external force F_l at the carriage, which can be considered as an equivalent external torque at the screw. For design details the reader may refer to [2].
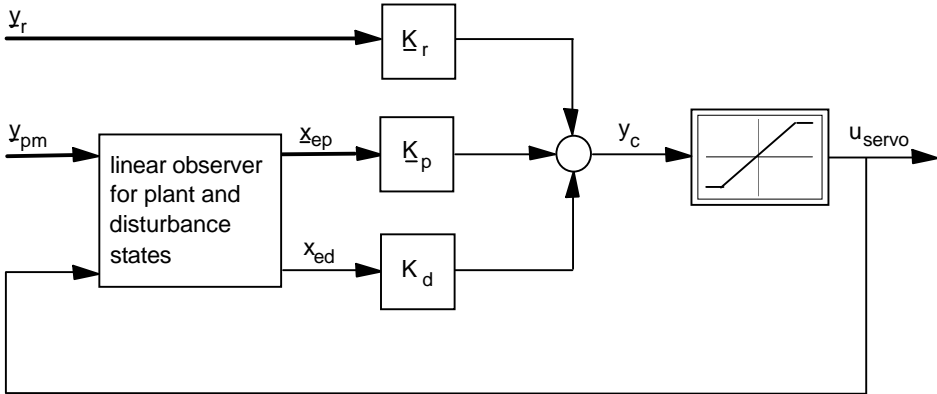

Fig. 11 *Compensator with linear model-based disturbance estimation and feedforward*

Tracks I and II commanded to the control system with the above compensator produced the position error measurements from figure 12. Again, the position error reaches its maximum after rapid changes of friction with the start of motion from standstill and with the motion reversal.
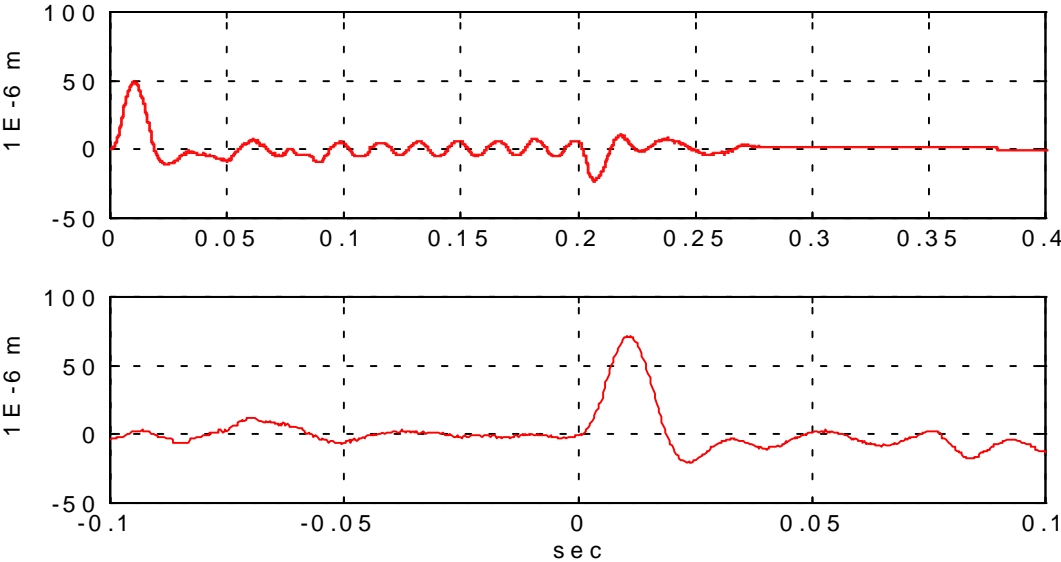
Fig. 12 *Positioning errors for track I (top) and II (bottom), compensator with linear model-based disturbance estimation and feedforward*

On a first look, compared to the results from the integral feedback in section 2.1, the improvements seem not to be dramatic. Disturbance feedforward results in slightly decreased peak values of the position errors and smaller fall times, i.e. the times the errors take to get from their peak values to zero the first time, especially for track II with the motion reversal and associated sign change of static friction. However, disturbance feedforward shows a strong

rejection to external disturbances, as it becomes clear by the fast decay of the simulated position error from a disturbance input step in figure 13.
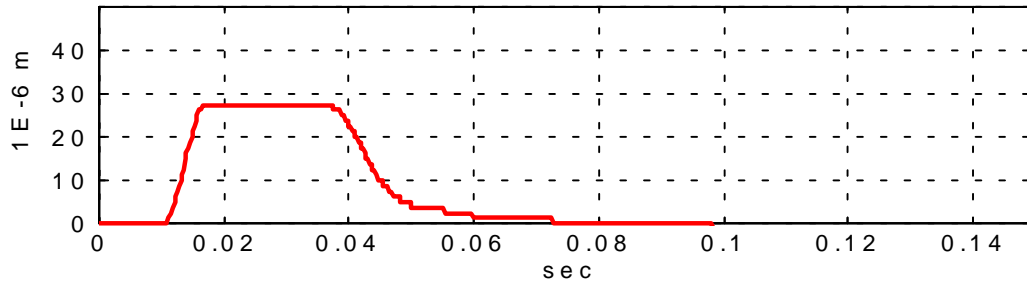

Fig. 13 *Position error for force step input, compensator with linear model-based disturbance estimation and feedforward*

Regarding the robustness of the nonlinear control system against changes of friction characteristics, it was not possible to produce a limit cycle in the simulation, even with unfavourable friction parameters. Also its robustness against variation of the load-side inertia and stiffness of the coupling turned out to be very good.

The robustness of the linear control system against disturbances and uncertainties in the plant control input path again is expressed by the open-loop bode plots for the system with LQR and LQG compensator from figure 14. LTR is nearly achieved.
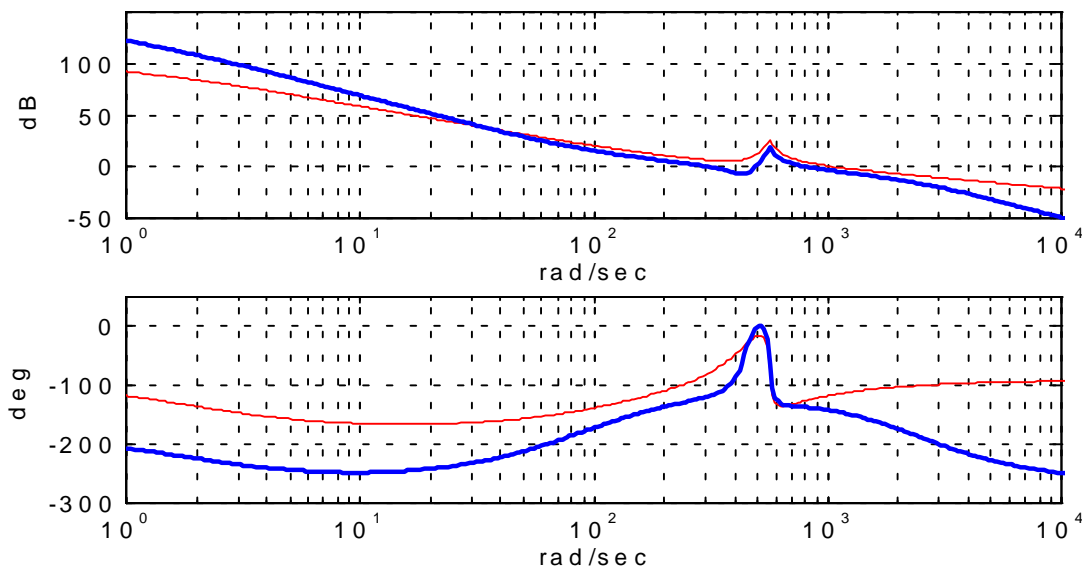

Fig. 14 *Open-loop bode plots for system with LQR (thin lines) and compensator with linear model-based disturbance estimation and feedforward (bold lines)*

2.3 Disturbance estimation and feedforward with residual

A drawback of the previous control schemes is the delayed generation and feedforward of the signal for friction compensation from the integrator or disturbance model in the observer. A promising approach to increase the speed of disturbance estimation and to decrease the position error peak values is suggested in [8]. It uses the residual vector

$$\underline{r} = \underline{y}_{pm} - \underline{y}_{em} = \underline{C}_{pm}\left(\underline{x}_p - \underline{x}_{ep}\right) = \underline{C}_{pm}\,\underline{e} \qquad (1)$$

with the original and estimated measurement vectors $\underline{y}_{pm}$ and $\underline{y}_{em}$, the plant measurement matrix $\underline{C}_{pm}$, and the plant state $\underline{x}_p$ and its estimate $\underline{x}_{ep}$, to estimate a constant external disturbance vector to the plant

$$\underline{u}_{epd} = \underline{M}\cdot\underline{r} \qquad (2)$$

by multiplying the residual vector by a constant disturbance filter matrix $\underline{M}$. A derivation is given in appendix C. This method to reconstruct an external disturbance input assumes a constant (non-zero) steady-state residual $\underline{r}$ and estimation error $\underline{e}$, which results in the following drawbacks. A non-zero estimation error contradicts the goal with the use of an observer, i.e. to get an error-free estimate of the plant states. With the tracks commanded to the EMPS, which produce rapid changes of the values of friction, with external forces acting at the carriage as well as process and measurement noise exciting the controlled system, also the assumption of a constant disturbance input and steady-state estimation error ($\dot{e} = 0$) is hardly to hold. Finally the approach is extremly sensitive to measurement noise. This is due to the direct feedthrough of the noisy measurement vector $\underline{y}_{pm}$ to the disturbance estimate u_{epd} and to the control signal u_{servo} by the disturbance feedforward gain K_d. Despite the direct feedthrough of the measurement vector to the disturbance estimate, the separation theorem holds, and the LQR and LQE can be separately designed as usual. However, the resulting LQG compensator for the EMPS with estimation of the load-side friction torque corresponding to the above formulas and its compensation by the feedforward gain K_d showed a very poor LTR of the linear control system. Simulation of the nonlinear system proved its poor robustness against measurement noise, especially against noise and ripple on the tachometer signal. Without measurement disturbances, while tracking, the steady-state estimation error in the state vector feedback produced a considerable steady-state positioning error which varied with the level of the kinetic friction. Additionally, the simulation showed limit cycles around standstill. The real system became unstable, thus no useful results could be achieved in the experiment. This behaviour could not be improved by the sole use of the less disturbed residual of the load-side position mesaurement for friction compensation.

In [9] the combination of the above residual-based and the linear model-based estimation and feedforward from section 2.2 is suggested for friction compensation. This gives remedy to the undesired steady-state estimation error with the purely residual-based approach. Figure 15 illustrates the associated compensator structure with the plant measurement matrix $\underline{C}_{pm}$ and the disturbance filter matrix $\underline{M}$. As in section 2.2 the observer for the plant and disturbance states is given by equations (A4a-c) from the appendix.
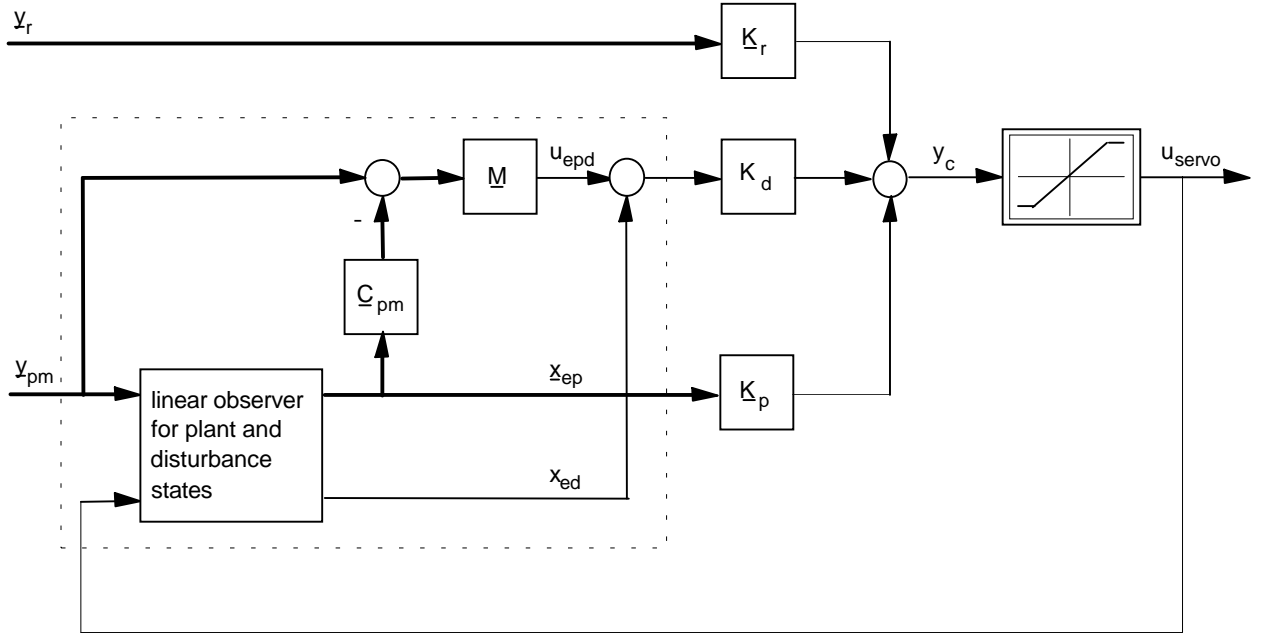
Fig. 15 *Compensator with residual-based plus linear model-based disturbance estimation and feedforward (observer with direct feedthrough in dashed frame)*

While the residual-based disturbance estimation shows a fast reaction and is effective at small times, the model-based estimation becomes active at larger times with the estimation error and the residual-based estimate tending to zero [9]. Due to the use of the residual vector, the observer for the plant state and friction (blocks in the dashed frame) again has a direct feedthrough (without filtering) and amplification of the measurement noise to the control signal. When the filter matrix $\underline{M}$ for the residual-based estimate is designed for the two residuals of the tachometer and incremental encoder measurements and a load-side disturbance input u_{pd} for friction and the force F_l , the control produces an awful position error for any track commanded to the system. Simulation revealed that this is mainly caused by the noise and ripple on the tachometer signal, and to a minor degree by the servo amplifier noise and the quantization of the encoder signal. Also this control system has a poor LTR and shows limit cycles around standstill.

The effect of tachometer noise to the control signal could be eliminated by only using the residual of the position measurement for the fast reconstruction of the load-side friction. Equation (2) then becomes

$$u_{epd} = \begin{bmatrix} 0 & m \end{bmatrix} \cdot \underline{r} = \begin{bmatrix} 0 & m \end{bmatrix} \cdot (\underline{y}_{pm} - \underline{C}_{pm} \underline{x}_{ep}) \quad , \tag{3}$$

where m is

$$m = (\underline{c}_{incr}^{T} (\underline{L}_p \underline{C}_{pm} - \underline{A}_p)^{-1} \underline{b}_{pd})^{-1} \quad . \tag{4}$$

In (4) $\underline{A}_p$ is the dynamic matrix, $\underline{b}_{pd}$ the column of the input matrix which corresponds to the external disturbance input u_{pd} , and $\underline{c}_{incr}^{T}$ is the row from the measurement matrix of the linear plant model producing the position measurement output incr. $\underline{L}_p$ is the submatrix from the augmented plant observer gain matrix coupling the residuals to the plant states (see appendix C).

With the residual-based disturbance estimation from equations (3) and (4), the robustness of the linear system recovers, which becomes evident by LTR bode plots close to those from figure 14, but with a slightly lower phase. However, simulation showed a high sensitivity of the nonlinear control system to a variation of the stiffness of the coupling when friction was present in the plant model. A reduction of the stiffness by 20% already resulted in instability. For re-stabilization, the disturbance filter gain m had to be reduced to 70% of the nominal value from design. For a stable experiment even a reduction of more than 50% was neccessary. This reduction strongly depended on the actual friction characteristic which varies with temperature and other environmental conditions. Althoug the real system was stable with the reduced disturbance filter gain, it still was very sensitive. This was indicated by vibrations which occurred in the experiment when the ball screw was tried to be clamped or twisted manually. Around standstill limit cycles occured in the experiment and simulation, which by simulation turned out to be strongly dependent on friction and other plant parameters. Figure 16 presents the best results which could be achieved with the compensator from figure 15 for tracks I and II.
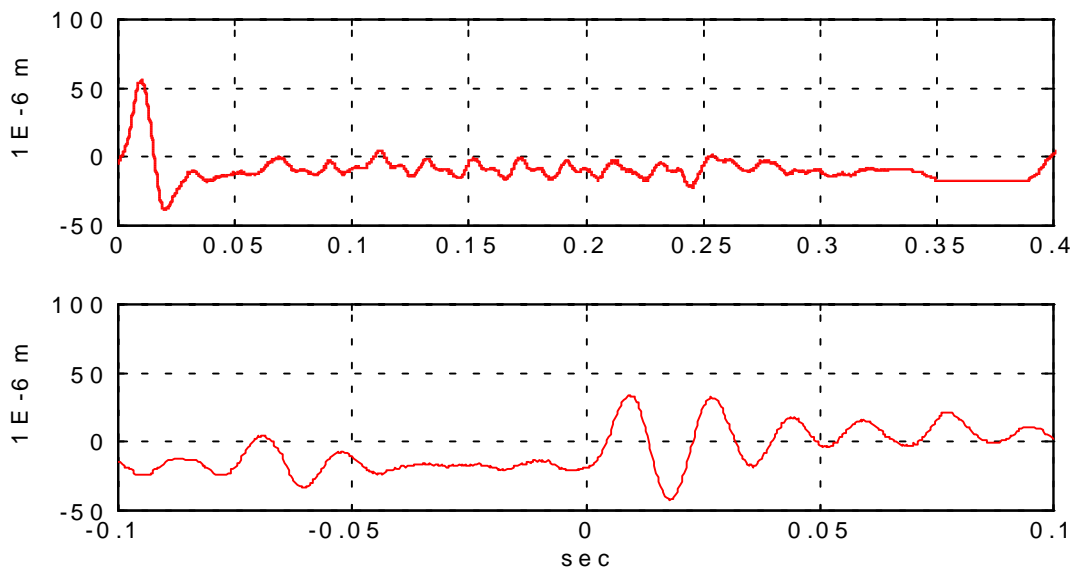

Fig. 16 *Positioning errors for track I (top) and II (bottom), compensator with residual- plus linear model-based disturbance estimation and feedforward*

In addition to the poor robustness of the nonlinear control system with friction and the limit cycles, the above error measurements represent no improvement compared to the results achieved with the purely linear model-based disturbance estimation from figure 12. Therefore the residual-based approach for friction estimation is considered to be less useful for highly dynamical and precise position control of the EMPS. Also, due to the observer error dynamics, with step like changes the valid friction estimates are still delayed. Thus, further potential to improve the compensation is given by a better reconstruction of the sign change of friction with the motion reversal of track II.

2.4 Nonlinear model-based disturbance estimation and feedforward

An idea to overcome the drawbacks of the previous compensation schemes from delayed feedforward and noisy estimates of the disturbing friction is to approximately pre-compensate the friction in the plant by the use of a nonlinear friction model. Since the reconstruction of the sign change of friction at zero velocity is of major interest, a simple model should be sufficient. The slow changes of friction with velocity can still be estimated following the linear model-based approach from section 2.2. This should yield further reduction of the position error, when the drive starts to move from standstill with track I and especially for the motion reversal of track II. Figure 17 shows the selected compensator structure.
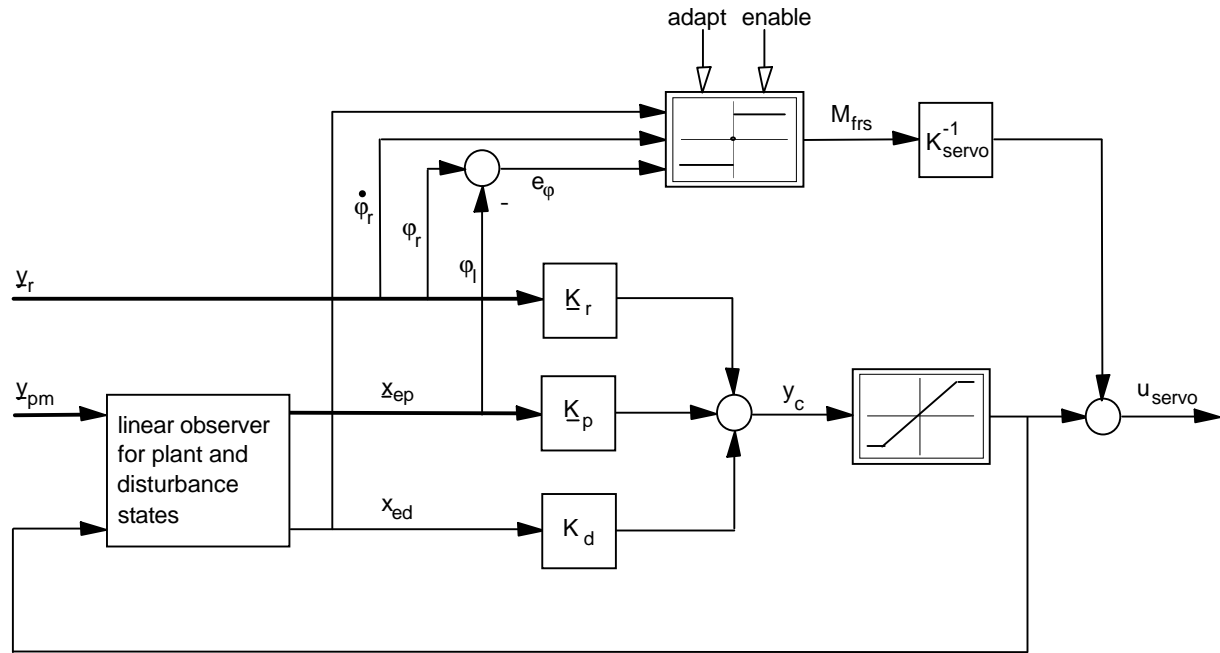

Fig. 17 *Compensator with nonlinear model-based disturbance estimation and feedforward*

The pre-compensation of the friction torque in the EMPS is performed by feedforward of the nonlinear friction model output M_{frs} . For a positive or negative reference velocity $\dot{\varphi}_r$, this signal is the positive or negative break-away (static) friction torque M_{S+} or M_{S-} , respectively. If zero reference velocity is commanded to the system, M_{frs} is set to M_{S+} , M_{S-} or zero depending on whether the load-side position error e_φ is positive, negative or zero. The reciprocal of the servo amplifier gain k_{servo} (gain between input voltage u_{servo} and motor torque M_d) serves to adjust the torque M_{frs} to the control signal. To avoid undesired switching of the nonlinear friction output, the reference velocity instead of a noisy measurement signal is used as input to the friction model. This substitution is possible due to the sufficiently strong position feedback and the feedforward of the reference and disturbance signals, which lets the load-side plant states closely follow the reference signals. The above pre-compensation relieves the linear model-based estimation and feedforward in the way that this has only to compensate for a smaller remaining disturbance seen by the linear observer for the plant and disturbance states (see appendix A).

A good knowledge of the break-away friction torques M_{S+} and M_{S-} is crucial for a proper operation of the above scheme. These parameters of the nonlinear friction model have to be adapted to the real values which vary with the operating condition of the EMPS. This is done with the aid of the linear model-based disturbance estimate x_{ed} as a third input to the friction

model. The adaption procedure for M_{S+} and M_{S-} can easily be explained with the flow chart shown in figure 18.
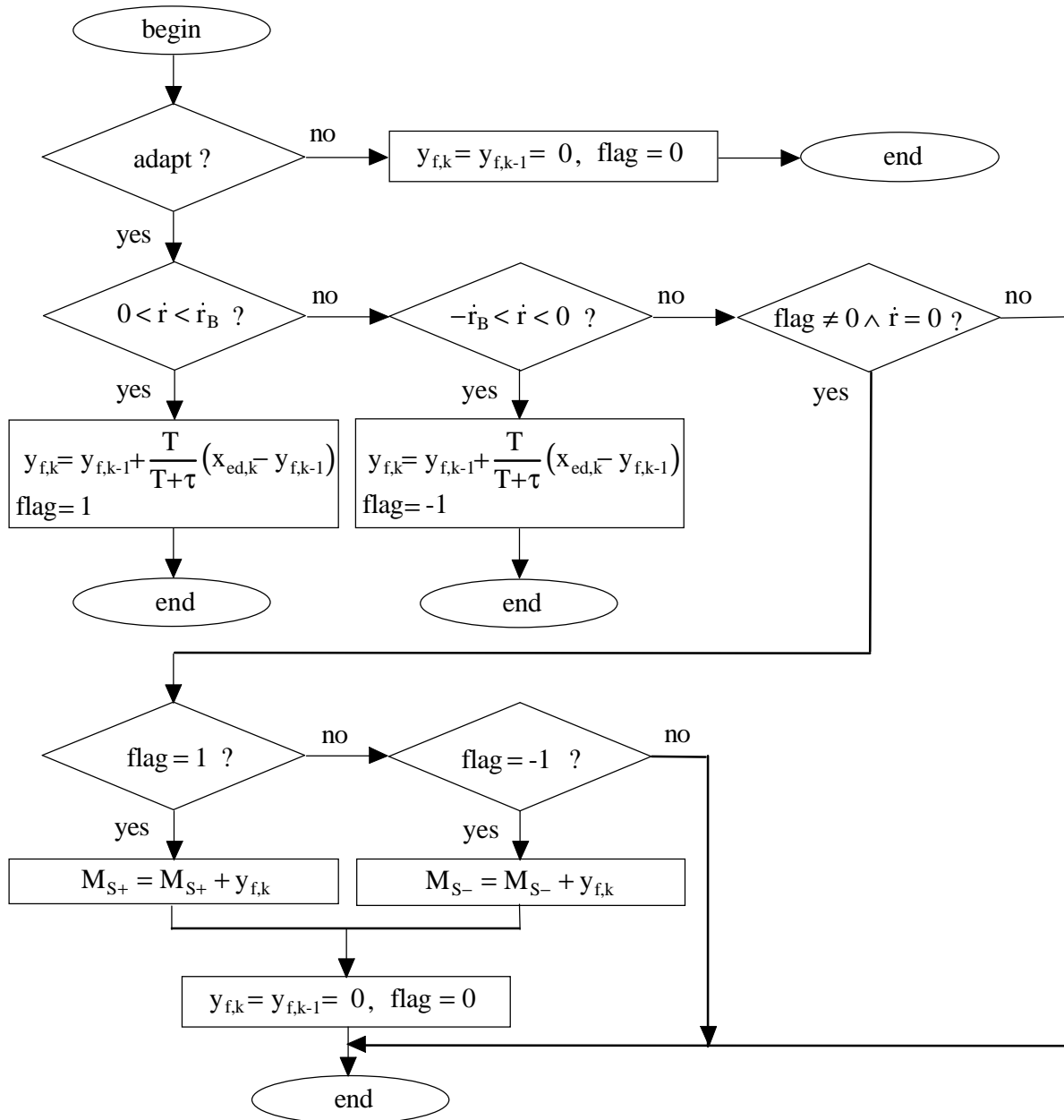

Fig. 18 *Flowchart of friction model parameter adaption*

The algorithm described by the flow chart is executed every sampling period T. If the reference velocity $\dot{r} = \dot{\phi}_r$ is in a specified interval $(-\dot{r}_B, \dot{r}_B)$ around zero, but not equal to zero, and the carriage is decelerating, the estimate x_{ed} will be taken to update a discrete first order lag with time constant τ for the positive or negative break-away friction torque, respectively. This filtering is required to suppress the noise contained in the friction estimate and to obtain smooth steady-state values for M_{S+} and M_{S-}. A flag indicates which of the friction torques is addressed. The filtering finishes as soon as the velocity input becomes zero. From now a new friction value becomes effective for pre-compensation by updating the respective positive or negative torque M_{S+} or M_{S-}. This update at standstill avoids an undesired dynamic effect of the adaption process to the control system. Finally the flag and the filter state are reset for the next adaption procedure. The update of M_{S+} and M_{S-} is done by adding the filter output y_f to the

respective previous value of M_{S+} or M_{S-}, which results in a decreasing estimate x_{ed} until the break-away torques have reached their steady states. Also, as already mentioned, the adaption is only performed during deceleration of the carriage, controlled by the input *adapt* to the nonlinear friction block in figure 17. This ensures that the friction estimate x_{ed} from the observer has settled. Another advantage with a hysteresis from frictional memory is that lower values for the break-away friction are identified and no over-compensation occurs in the acceleration phase. The adaption process can be disabled and the nonlinear friction output can be set to zero by the *enable* input to the friction block.

Figure 19 shows the time histories for the adaption of M_{S+} and M_{S-} starting from their initial values with a particular tracking of the carriage. The steady-state values are good estimates for the break-away friction torques evaluated from the measurement given by figure 2.
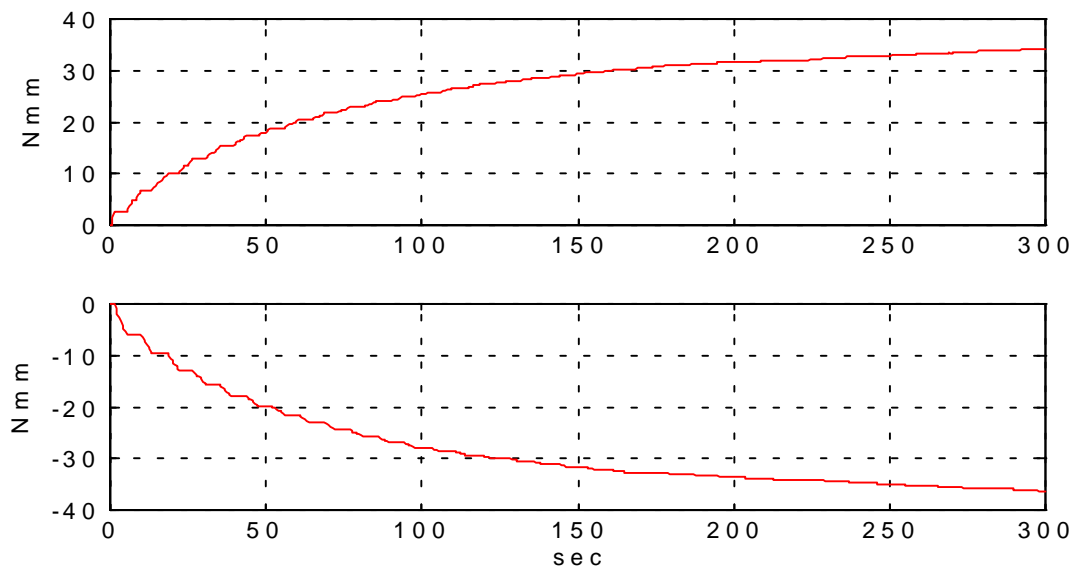

Fig. 19 *Adaption of M_{S+} (top) and M_{S-} (bottom), $\tau=0.5$ sec, $\dot{r}_B = 50$ rad/sec ($\approx$ 0.02 m/sec carriage velocity)*

The bold lines in the plots of figure 20 are the friction torque estimates of the compensator with and without nonlinear friction model for track II. With the model, the estimate is the sum of its output M_{frs} (straight thin line) and the observer disturbance estimate x_{ed} (noisy thin line). While without the nonlinear model the estimate changes slowly with the motion reversal at time t = 0.0 sec, the sign change of the friction is well reconstructed with the model contained in the compensator. The offset of about 20 Nmm in the friction estimate can be explained by offset voltages in the analog servo amplifier and a mismatch of the moments of inertia in the real EMPS and the linear EMPS model used for observer design [9].
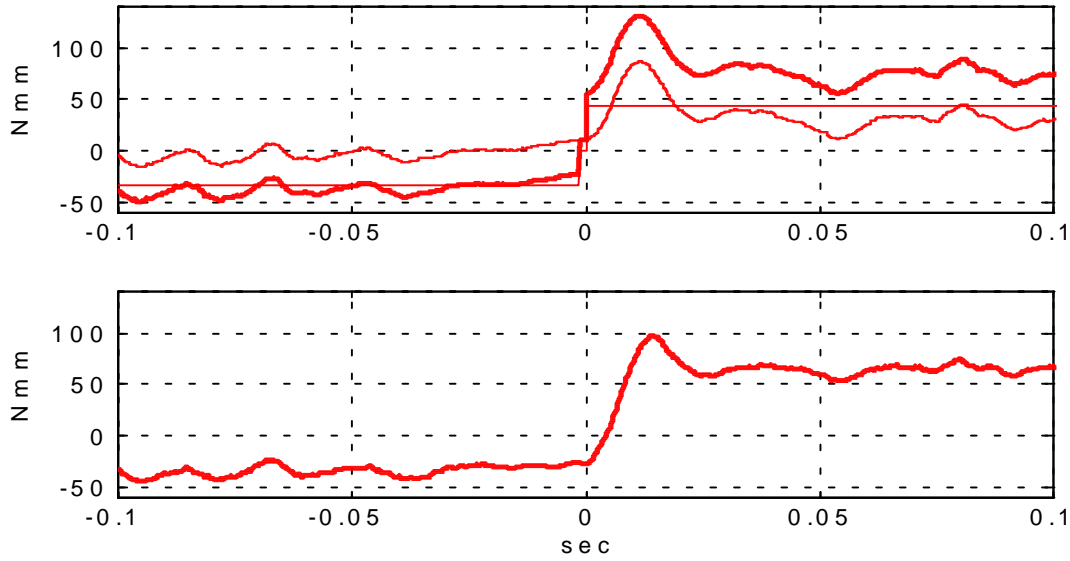
Fig. 20 *Friction torque estimates from compensator with (top) and without (bottom) nonlinear friction model*

Corresponding to the improved friction estimate with the nonlinear friction model, compared to the results from section 2.2 the position error measurements present a decrease of their peak values and fall times. As can be seen in figure 21, this improvement is only marginal for track I with a slightly decreased fall time of the peak error from the first acceleration step. Due to the reconstruction of the sign change of friction with the motion reversal, the position error for track II, however, shows a significantly decreased peak value and fall time.
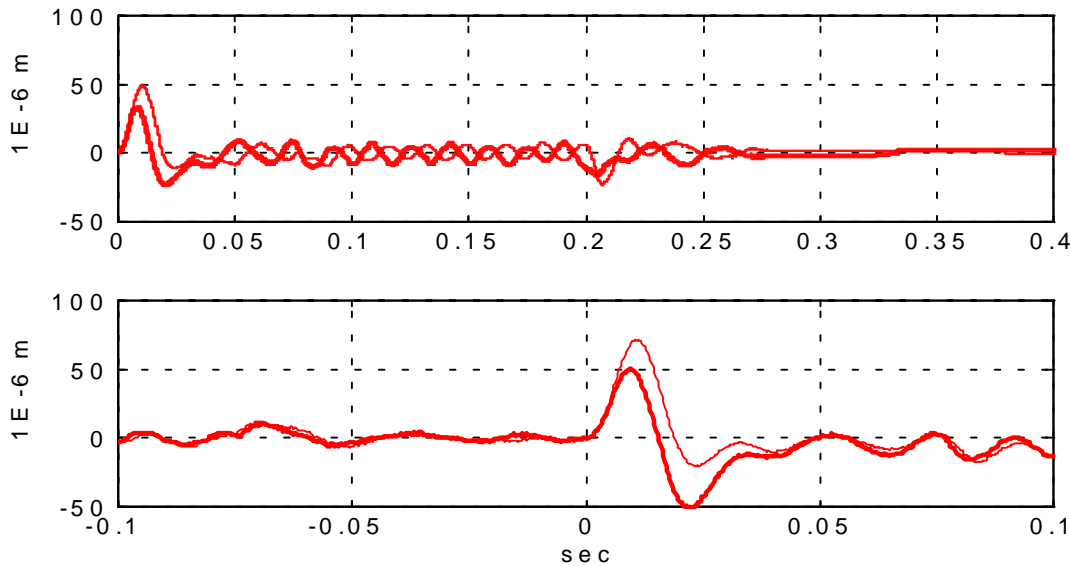
Fig. 21 *Positioning errors for track I (top) and II (bottom), compensator with nonlinear model-based disturbance estimation and feedforward (bold lines), compensator with linear model-based disturbance estimation from section 2.2 (thin lines)*

The improvement increases with higher friction torques in the EMPS and lower bandwidth of the disturbance observer, which may be imposed for cost reasons by less quality mechanical components or a slower hardware for compensator implementation. The results in figure 22

demonstrate the case that the bandwidth of the disturbance observer is only about two times lower. In this case the improvement also becomes visible for track I in a smaller peak value and fall time of the error from the first acceleration step.
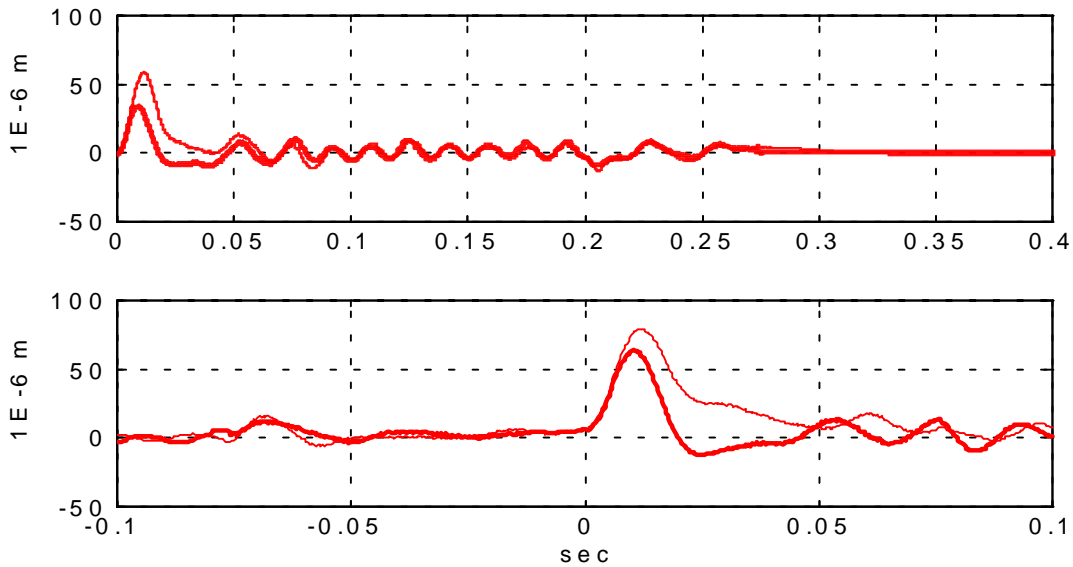
Fig. 22 *Positioning errors for track I (top) and II (bottom), same compensators as for figure 21 , bandwidth of disturbance observer two times lower*

Since for zero reference velocity the nonlinear friction model output M_{frs} depends on the load-side position error e_φ , the pre-compensation of friction is also effective with pure disturbance excitation of the EMPS from the external force F_l . This is due to the fast overcomming of the break-away friction torque in the EMPS by the friction model output in the control signal. As can be seen from the simulation result in figure 23, the position error due to a force step input has a smaller peak value and settling time when the nonlinear friction model is included in the compensator. This improved disturbance behaviour of the control system can also be recognized in the experiment when one tries to twist the screw manually.
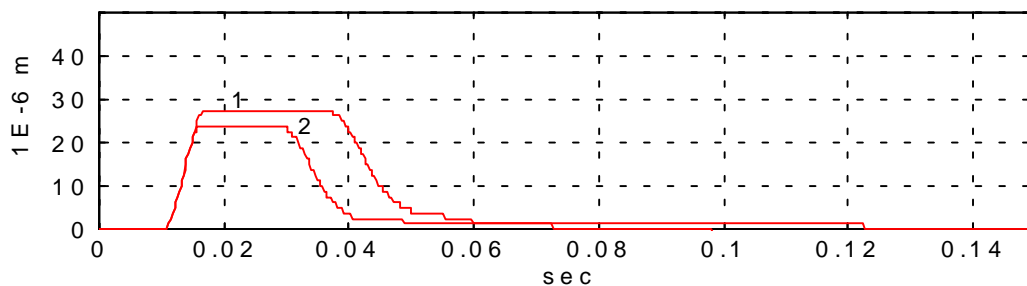
**Fig. 23** *Position error for force step input, compensator with nonlinear model-based disturbance estimation and feedforward (1), compensator with linear model-based disturbance estimation from section 2.2 (2)*

If the EMPS is operating under varying forces F_l , the adaption procedure for the friction model should be performed only during force free tracking (e.g. during special learning phases), which can be controlled by the *adapt* input. This avoids that the load force is misinterpreted as friction which would result in over-compensation when the force becomes zero.

All simulation and experimental results showed that the robustness of the control system retained the very good properties of the system from section 2.2 .

Another compensator structure which was investigated for nonlinear model-based disturbance estimation and feedforward is given in figure 24. Here the nonlinear friction model is included in the observer by injection of its output M_{frs} to the additional nonlinear function input $f_d(.)$ to the observer. A general derivation of the resulting nonlinear observer is given in appendix B. This approach is the obvious extension of the linear model-based approach and is strictly following the observer theory. In comparison to figure 20 the resulting friction torque estimate does not show the large overshoot after step-like changes of the friction torque and thus yields a better estimate for the friction in the plant than the more intuitive approach with the structure from figure 17. In difference to figure 17 now both parts of the estimate are fed forward to the compensator output y_c by the same disturbance feedforward gain K_d and are contained in the plant control signal which is fed back to the observer.
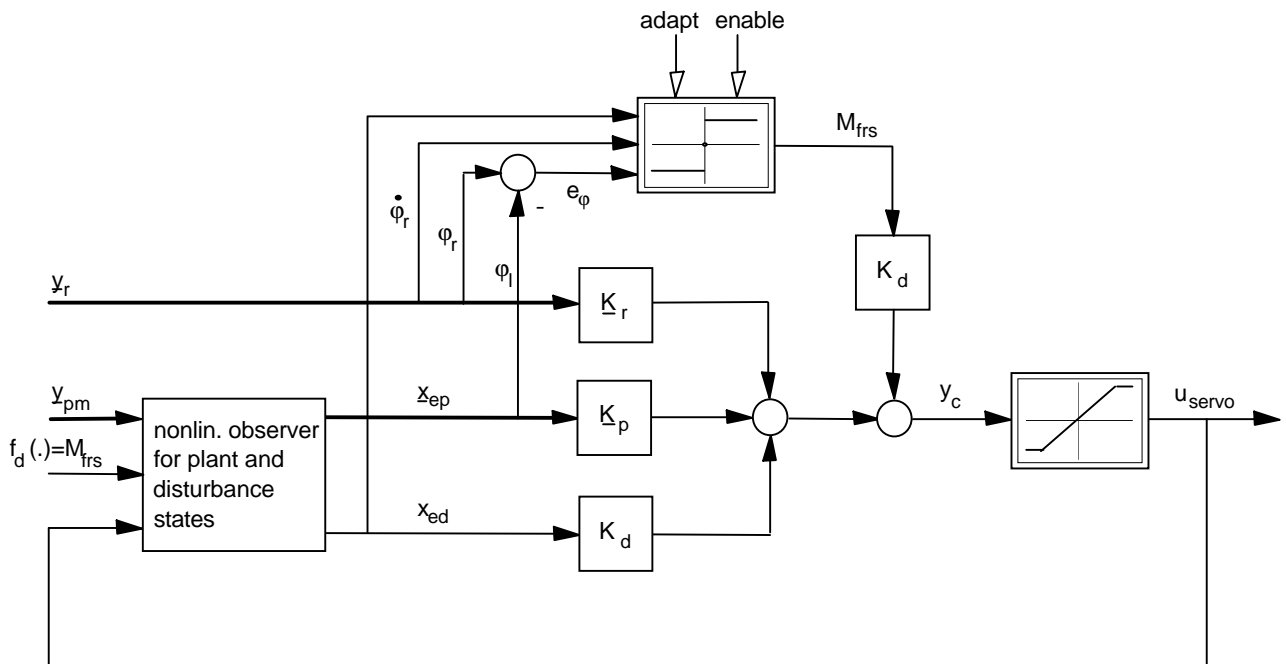
Fig. 24 *Compensator with nonlinear model-based disturbance estimation and feedforward, nonlinear friction model included in the observer*

Compared to the results with the compensator from figure 17 for tracks I and II, the closed loop system with the above compensator shows slightly smaller peak values of the position errors but larger fall times. This becomes especially clear by comparing the force step responses shown in figure 25. The smaller error fall times with the compensator from figure 17 can be explained by the overshoot in the friction torque estimate with step-like changes of the friction torque (figure 20), which yields a stronger reaction to disturbing torques resulting in a faster decay of the corresponding postion errors. Since this rejectiveness to disturbing torques is considered more important for the EMPS control, the compensator from figure 17 has been preferred to that from figure 24.
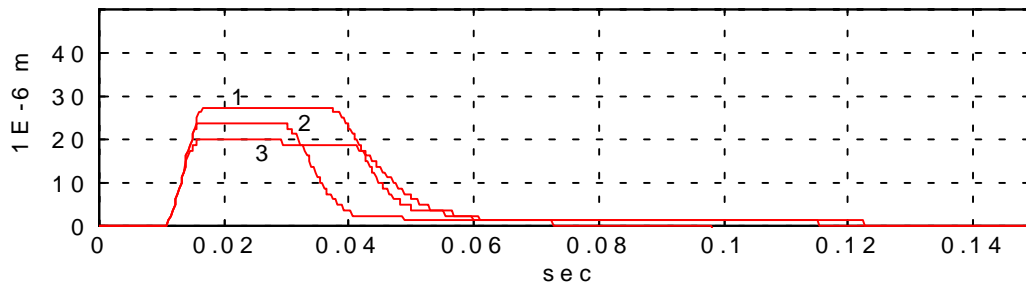
Fig. 25 *Position errors for force step input, compensator from section 2.2 (1), compensator from figure 17 (2), compensator from figure 24 (3)*

3. Conclusions

A selection of friction compensation schemes for highly dynamical and precise position control of an EMPS with compliance and friction have been experimentally studied with regard to their reference and disturbance behaviour and robustness. The schemes originate from a simple LQG control and differ by the type of augmentation for the estimation of load-side friction torque and disturbing forces and the compensation of the resulting position errors.

The first approach, an integral feedback of the position error, provides a satisfactory reference behaviour, but week disturbance rejection. It shows a good robustness against noise and model uncertainties and is a feasible solution if the sources of position errors are not well known or cannot be modelled, which is not the case in the considered application.

Linear model-based disturbance estimation and feedforward, a linear integrator disturbance model in the observer and feedforward of the corresponding state as an estimate for friction, yields a slightly improved reference behaviour and a strong rejection of external disturbances. It also shows a good robustness against noise and modelling errors.

An attempt to decrease the lag and delayed feedforward of the friction estimate by a residual-based approach for disturbance estimation has not yielded the expected results for the EMPS. This is due to the poor robustness of this scheme against measurement noise and plant parameter variations. Also limit cycles could be recognized during simulation of the nonlinear control system with friction as well as in the experiment.

Due to its capability to reconstruct the sign change of friction with motion reversal, the best results for both, reference profile tracking and disturbance rejection, are achieved with a nonlinear adaptive friction model in the compensator. The resulting scheme comprises a combination of linear and nonlinear model-based disturbance estimation and retains the good robustness properties of the linear model-based approach. It is even more promising if high friction or low observer dynamics are imposed by less quality mechanical components or a low-speed hardware for digital compensator implementation.

To relieve the user of design and real-time programming details, the design and implementation of all compensation schemes has been automated by the aid of interactive user interfaces with MATLAB/SIMULINK and the dSPACE TDE.

Appendix

To get a more general derivation of the different principles of disturbance estimation treated in this paper, we assume a plant model with direct feedthrough of the control and disturbance input vectors to the measurement output vector. This feedthrough is given in equation (A1) by the matrices $\underline{D}_{pmc}$ and $\underline{D}_{pmd}$ and may occur when acceleration measurements are among the measurement signals. The observer equations derived in the following appendix sections are contained in the observer blocks shown in the compensator structures for the EMPS control in section 2. However, with its drive-side angular velocity and load-side position measurements the EMPS does not have the direct feedthrough and the resulting zero matrices $\underline{D}_{pmc}$ and $\underline{D}_{pmd}$ have been dropped. This particular case is mostly considered in the literature.

A Linear model-based disturbance estimation

Given the state equations of a linear plant model

$$
\begin{aligned}
\dot{\underline{x}}_p &= \underline{A}_p \underline{x}_p + \underline{B}_{pc} \underline{u}_{pc} + \underline{B}_{pd} \underline{u}_{pd} \\
\underline{y}_{pm} &= \underline{C}_{pm} \underline{x}_p + \underline{D}_{pmc} \underline{u}_{pc} + \underline{D}_{pmd} \underline{u}_{pd}
\end{aligned}
\tag{A1}
$$

with the control input vector $\underline{u}_{pc}$, the disturbance input vector $\underline{u}_{pd}$ and the measurement output vector $\underline{y}_{pm}$. If the disturbance input of the plant $\underline{u}_{pd}$ can be approximated by the output $\underline{y}_d$ of the linear model

$$
\begin{aligned}
\dot{\underline{x}}_d &= \underline{A}_d \underline{x}_d \quad , \qquad \underline{x}_d (t = 0) = \underline{x}_{d0} \\
\underline{y}_d &= \underline{C}_d \underline{x}_d
\end{aligned}
\tag{A2}
$$

with appropriate initial condition for the state, by substitution $\underline{u}_{pd} = \underline{y}_d$ the correspondig augmented plant model becomes

$$
\begin{aligned}
\dot{\underline{x}} &= \underline{A} \, \underline{x} + \underline{B} \, \underline{u}_{pc} \\
\underline{y}_{pm} &= \underline{C} \, \underline{x} + \underline{D} \, \underline{u}_{pc}
\end{aligned} \quad ,
\tag{A3a}
$$

where the augmented plant state vector and state space matrices with appropriate dimensions are

$$
\underline{x} = \begin{bmatrix} \underline{x}_p \\ \underline{x}_d \end{bmatrix}, \qquad \underline{A} = \begin{bmatrix} \underline{A}_p & \underline{B}_{pd} \underline{C}_d \\ \underline{0} & \underline{A}_d \end{bmatrix}, \quad \underline{B} = \begin{bmatrix} \underline{B}_{pc} \\ \underline{0} \end{bmatrix}
$$
$$
\underline{C} = \begin{bmatrix} \underline{C}_{pm} & \underline{D}_{pmd} \underline{C}_d \end{bmatrix}, \, \underline{D} = \underline{D}_{pmc}
\tag{A3b}
$$

The state vector (plant and disturbance states) of this augmented system can be estimated by the linear observer

$$\dot{\underline{x}}_e = \underline{A}\,\underline{x}_e + \underline{B}\,\underline{u}_{pc} + \underline{L}\,(\underline{y}_{pm} - \underline{y}_{em})$$
$$= (\underline{A} - \underline{LC})\,\underline{x}_e + (\underline{B} - \underline{L}\,\underline{D})\,\underline{u}_{pc} + \underline{L}\,\underline{y}_{pm}$$
$$= \underline{A}_e\,\underline{x}_e + \underline{B}_e\,\underline{u}_e$$
$$\underline{y}_e = \underline{x}_e$$

(A4a)

with the input and state vectors

$$\underline{u}_e = \begin{bmatrix} \underline{u}_{pc} \\ \underline{y}_{pm} \end{bmatrix}, \quad \underline{x}_e = \begin{bmatrix} \underline{x}_{ep} \\ \underline{x}_{ed} \end{bmatrix} \quad .$$

(A4b)

By partitioning the observer gain matrix into submatrices $\underline{L} = \begin{bmatrix} \underline{L}_p \\ \underline{L}_d \end{bmatrix}$ corresponding to the plant and disturbance model substates in the augmented state vector, the state space matrices of the augmented plant observer can be determined as

$$\underline{A}_e = \underline{A} - \underline{LC} = \begin{bmatrix} \underline{A}_p - \underline{L}_p\underline{C}_{pm} & (\underline{B}_{pd} - \underline{L}_p\underline{D}_{pmd})\,\underline{C}_d \\ -\underline{L}_d\underline{C}_{pm} & \underline{A}_d - \underline{L}_d\underline{D}_{pmd}\underline{C}_d \end{bmatrix}$$

$$\underline{B}_e = \begin{bmatrix} \underline{B} - \underline{LD} & \underline{L} \end{bmatrix} = \begin{bmatrix} \underline{B}_{pc} - \underline{L}_p\underline{D}_{pmc} & \underline{L}_p \\ -\underline{L}_d\underline{D}_{pmc} & \underline{L}_d \end{bmatrix}$$

(A4c)

B Nonlinear model-based disturbance estimation

If an advance estimate $\hat{\underline{u}}_{pd}$ of the disturbance input to the plant model from equation (A1) is given as a nonlinear function $\hat{\underline{u}}_{pd} = \underline{f}_d(.)$ of other control system variables, it can be used to improve the estimates from the augmented plant observer from appendix A. This is done by adding the function value to the linear model approximation of the disturbance signal from equation (A2):

$$\underline{y}_d = \underline{C}_d\,\underline{x}_d + \underline{f}_d(.) \quad .$$

(B1)

The function can be considered as an external input to the augmented plant model from (A3a), which then becomes

$$\dot{\underline{x}} = \underline{A}\,\underline{x} + \underline{B}\,\underline{u}_{pc} + \underline{E}\,\underline{f}_d(.)$$
$$\underline{y}_{pm} = \underline{C}\,\underline{x} + \underline{D}\,\underline{u}_{pc} + \underline{F}\,\underline{f}_d(.) \quad ,$$

(B2a)

where

$$\underline{E} = \begin{bmatrix} \underline{B}_{pd} \\ \underline{0} \end{bmatrix} \quad \text{and} \quad \underline{F} = \underline{D}_{pmd} \quad .$$

(B2b)

The augmented plant state vector and remaining state space matrices are given in equation (A3b). This system entered to an observer design results in the nonlinear observer

$$\dot{\underline{x}}_e = (\underline{A} - \underline{L}\underline{C})\,\underline{x}_e + (\underline{B} - \underline{L}\underline{D})\,\underline{u}_{pc} + \underline{L}\,\underline{y}_{pm} + (\underline{E} - \underline{L}\underline{F})\,\underline{f}_d(.)$$
$$= \underline{A}_e\,\underline{x}_e + \underline{B}_e\,\underline{u}_e \qquad . \qquad\qquad (B3a)$$
$$\underline{y}_e = \underline{x}_e$$

Since the nonlinear function $\underline{f}_d(.)$ is known, it has been added to the observer input vector

$$\underline{u}_e = \begin{bmatrix} \underline{u}_{pc} \\ \underline{y}_{pm} \\ \underline{f}_d(.) \end{bmatrix} \quad , \qquad\qquad (B3b)$$

so that the correponding observer input matrix becomes

$$\underline{B}_e = \begin{bmatrix} \underline{B} - \underline{L}\underline{D} & \underline{L} & \underline{E} - \underline{L}\underline{F} \end{bmatrix} = \begin{bmatrix} \underline{B}_{pc} - \underline{L}_p\underline{D}_{pmc} & \underline{L}_p & \underline{B}_{pd} - \underline{L}_p\underline{D}_{pmd} \\ -\underline{L}_d\underline{D}_{pmc} & \underline{L}_d & -\underline{L}_d\underline{D}_{pmd} \end{bmatrix} \quad . \qquad (B3c)$$

The state vector and system matrix of the nonlinear augmented plant observer can be taken from equations (A4b) and (A4c).

The estimate of the output of the linear disturbance model in the observer

$$\underline{y}_{ed} = \underline{C}_d\,\underline{x}_{ed} \qquad\qquad (B4)$$

obtained from the output equation in (A2) represents an estimate of the deviations of the real disturbance input to the plant from the nonlinear function value which is entered to the observer as an external input. While $\underline{y}_{ed}$ can be used to adapt the nonlinear function parameters, the disturbance model state $\underline{x}_{ed}$ together with the function output are feedforward signals in a control system with the plant model from equations (B2).

The design procedure for the above nonlinear observer needs the following steps. First a linear observer design is performed for the linear augmented plant model from (A3), which yields the gain matrix $\underline{L}$. Then the nonlinear observer is obtained with the matrices from equations (B3c) and (A4c) and the nonlinear function plugged into equations (B3a) and (B3b).

C Residual-based disturbance estimation [8,9]

Again given the plant model from equation (A1). With the linear observer

$$\dot{\underline{x}}_{ep} = (\underline{A}_p - \underline{L}_p\underline{C}_{pm})\,\underline{x}_{ep} + (\underline{B}_{pc} - \underline{L}_p\underline{D}_{pmc})\,\underline{u}_{pc} + \underline{L}_p\,\underline{y}_{pm} \qquad (C1)$$

used to estimate the plant states, the resulting error system becomes

$$\dot{\underline{e}} = \dot{\underline{x}}_p - \dot{\underline{x}}_{ep}$$
$$= (\underline{A}_p - \underline{L}_p\underline{C}_{pm})\,\underline{e} + (\underline{B}_{pd} - \underline{L}_p\underline{D}_{pmd})\,\underline{u}_{pd} \qquad (C2)$$

which shall be asymtotically stable by an appropriate design of the observer gain matrix $\underline{L}_p$. The estimation error is driven by the external disturbance input vector $\underline{u}_{pd}$. Assuming constant disturbance signals in $\underline{u}_{pd}$ and steady-state conditions ($t \to \infty$) the derivative of the estimation error in (C2) becomes zero

$$\underline{0} = (\underline{A}_p - \underline{L}_p \underline{C}_{pm}) \underline{e} + (\underline{B}_{pd} - \underline{L}_p \underline{D}_{pmd}) \underline{u}_{pd} \tag{C3}$$

which results in the constant steady-state estimation error

$$\underline{e} = (\underline{L}_p \underline{C}_{pm} - \underline{A}_p)^{-1} (\underline{B}_{pd} - \underline{L}_p \underline{D}_{pmd}) \underline{u}_{pd} \ . \tag{C4}$$

For an unique solution, we further assume that the number μ of measurement signals in the vector $\underline{y}_{pm}$ is greater than or equal to the number ν of disturbance inputs to the plant in the vector $\underline{u}_{pd}$. Be the steady-state estimate $\underline{u}_{epd}$ of the external disturbance input vector $\underline{u}_{pd}$ linearly dependent on the residual vector

$$\underline{r} = \underline{y}_{pm} - \underline{y}_{em} = \underline{y}_{pm} - \underline{C}_{pm} \underline{x}_{ep} - \underline{D}_{pmc} \underline{u}_{pc} = \underline{C}_{pm} \underline{e} + \underline{D}_{pmd} \underline{u}_{pd} \quad , \tag{C5}$$

which can be expressed by

$$\underline{u}_{epd} = \underline{M}\, \underline{r} \tag{C6}$$

with a suitable constant disturbance filter matrix $\underline{M}$ of size (ν,μ) , premultiplication of equation (C5) by $\underline{M}$ and substituting the steady-state estimation error from equation (C4) yields

$$\begin{aligned} \underline{u}_{epd} &= \underline{M}\,[\,\underline{C}_{pm} \underline{e} + \underline{D}_{pmd}\, \underline{u}_{pd}\,] \\ &= \underline{M}\,[\,\underline{C}_{pm}(\underline{L}_p \underline{C}_{pm} - \underline{A}_p)^{-1}(\underline{B}_{pd} - \underline{L}_p \underline{D}_{pmd}) + \underline{D}_{pmd}\,]\, \underline{u}_{pd} \end{aligned} \ . \tag{C7}$$

Additionally, in the steady state be $\underline{u}_{epd} = \underline{u}_{pd}$, this equation can be used to determine the disturbance filter matrix $\underline{M}$ from the relation

$$\underline{M}\,[\,\underline{C}_{pm}(\underline{L}_p \underline{C}_{pm} - \underline{A}_p)^{-1}(\underline{B}_{pd} - \underline{L}_p \underline{D}_{pmd}) + \underline{D}_{pmd}\,] = \underline{I}\ , \tag{C8}$$

where $\underline{I}$ is the (ν,ν)-identity matrix. Since with μ rows and ν columns and $\mu \geq \nu$ the matrix

$$\underline{N} = \underline{C}_{pm}(\underline{L}_p \underline{C}_{pm} - \underline{A}_p)^{-1}(\underline{B}_{pd} - \underline{L}_p \underline{D}_{pmd}) + \underline{D}_{pmd} \tag{C9}$$

in (C8) is not necessarily a square matrix, but shall be column regular, the disturbance filter matrix is the left inverse

$$\underline{M} = \left(\underline{N}^{\mathrm{T}} \underline{N}\right)^{-1} \underline{N}^{\mathrm{T}} = \underline{N}^{+} = \left(\underline{C}_{pm}(\underline{L}_p \underline{C}_{pm} - \underline{A}_p)^{-1}(\underline{B}_{pd} - \underline{L}_p \underline{D}_{pmd}) + \underline{D}_{pmd}\right)^{+} \ , \tag{C10}$$

where the superscripts T and + denote the transpose and left inverse of the matrix $\underline{N}$, respectively. With this $\underline{M}$ numerically determined from equation (C10) the observer for the

plant states with residual-based estimation of the constant disturbance input vector to the plant from (A1) becomes

$$
\begin{aligned}
\dot{\underline{x}}_{ep} &= \underline{A}_e \, \underline{x}_{ep} + \underline{B}_e \, \underline{u}_e \\
\underline{y}_e &= \underline{C}_e \, \underline{x}_{ep} + \underline{D}_e \, \underline{u}_e
\end{aligned}
\qquad . \tag{C11}
$$

With equations (C1), (C5) and (C6) the corresponding input and output vectors and state space matrices can be determined as

$$
\underline{u}_e = \begin{bmatrix} \underline{u}_{pc} \\ \underline{y}_{pm} \end{bmatrix} , \quad \underline{y}_e = \begin{bmatrix} \underline{x}_{ep} \\ \underline{u}_{epd} \end{bmatrix}
$$

$$
\underline{A}_e = \underline{A}_p - \underline{L}_p \underline{C}_{pm} , \quad \underline{B}_e = \begin{bmatrix} \underline{B}_{pc} - \underline{L}_p \underline{D}_{pmc} & \underline{L}_p \end{bmatrix} \qquad . \tag{C12}
$$

$$
\underline{C}_e = \begin{bmatrix} \underline{I} \\ -\underline{M}\,\underline{C}_{pm} \end{bmatrix} , \quad \underline{D}_e = \begin{bmatrix} \underline{0} & \underline{0} \\ -\underline{M}\,\underline{D}_{pmc} & \underline{M} \end{bmatrix}
$$

References

[1]   J.C. Doyle and G. Stein, Robustness with Observers. IEEE Transactions on Automatic Control, Vol. AC-24, 1979.

[2]   H. Henrichfreise, Prototyping of a LQG Compensator for a Compliant Positioning System with Friction. Paper at Cologne Laboratory of Mechatronics, FB KT, Polytechnic Cologne, 1996.

[3]   H.Hanselmann, DSP in Control: The Total Development Environment. International Conference on Signal Processing Applications & Technology ICSPAT'95, Boston, MA, USA, October 24-26, 1996.

[4]   B. Armstrong-Hélouvry, P. Dupont and Carlos Canudas de Wit, A Survey of Models, Analysis Tools and Compensation Methods for the Control of Machines with Friction. Automatica, Vol. 30, No. 7, 1994, pp. 1083-1138.

[5]   M. Wieland, Untersuchung des Einflusses einer dynamischen Bewertung der Entwurfszielgrößen beim LQR-Entwurf für eine Positionierregelung. Thesis for diploma degree at Cologne Laboratory of Mechatronics, FB KT, Polytechnic Cologne, 1996.

[6]   F. L. Lewis, Applied Optimal Control and Estimation. Prentice Hall, Englewood Cliffs, NJ, USA, 1992.

[7]   J. Ackermann and P.C. Müller, Dynamical behaviour of nonlinear multibody system due to Coulomb friction and backlash. Preprints of IFAC/IFIP/IMACS International Symposium on Theory of Robots, Wien 1986, pp. 289-295.

[8]   C. Bruce-Boye, Friction compensation via disturbance observer. Preprints of IFAC Symposium on Robot Control SYROCO'91, Wien 1991, pp. 359-362.

[9]   R. Neumann, Beobachtergestützte dezentrale entkoppelnde Regelung von Robotern mit elatischen Gelenken. Fortschritt-Berichte VDI, Reihe 8, Nr.529, VDI-Verlag, Düsseldorf 1996.